JOURNAL OF MATERIALS SCIENCE **30** (1995) 1203–1208

Silver–palladium submicronic powders

Part II *Structural characterization*

F. YALA*, E. DELARUE, M. O. DELCOURT
Laboratoire de Physico-Chimie des Rayonnements, CNRS URA 75, Bt 350, Université Paris-Sud, 91405 Orsay Cedex, France

C. HAUT, C. SEVERAC
Laboratoire de Métallurgie Physique, CNRS URA 1107, Bt 413, Université Paris-Sud, 91405 Orsay Cedex, France

C. GRATTEPAIN
Laboratoire de Physique des Solides de Bellevue, CNRS UPR 1332, 1 Place A. Briand, 92195 Meudon Cedex, France

The structure of new submicronic spherical Ag–Pd powders (75/25 and 70/30 wt/wt% as spheres of mean diameter ca. 300 nm) has been investigated by various techniques. X-ray diffraction, carried out on both powder and single particles, showed two distinct metal phases, the first one being pure silver, the second one slightly alloyed palladium. X-ray microanalysis performed under SEM indicated that each grain displays intermetallic character, both metals being present in proportion close to the mean composition. Space-resolved information has been obtained by three different techniques: X-ray microanalysis carried out under transmission electron microscopy, X-ray photoelectron spectroscopy and secondary ion mass spectrometry, the three of them leading to converging results. Each grain appears as a core made of pure silver surrounded by a 10–15 nm thick layer of slightly alloyed palladium with a mean Pd/Ag ratio 89%/11% which possibly increases from inside to outside.

1. Introduction

Intermetallic Ag–Pd powders are subject to increasing demands from the electronics industry [1–8] where they are used in multilayer ceramic chip capacitors to make thin conductive electrode films and termination inks. A point of major interest concerning these powders is the distribution of the metals in the submicronic particles of the powder. Only a true intermetallic character, i.e. the presence of both metals in each particle, as either fully alloyed or segregated in very small domains, can warrant the required performances (high conductivity, low thickness) for low-cost electrodes. In a previous paper [9], we have described the morphology and thermal properties of new Ag/Pd powders recently manufactured at CLAL by chemical reduction in aqueous solution. In the present paper, we investigate their structural properties, namely the distribution and arrangement of both metals inside the powder grains.

2. Experimental procedure

The powders from CLAL have a content Ag/Pd 75/25 or 70/30% wt/wt. They are made of spherical shaped grains (mean diameter 0.3 μm) [8] with low size-dispersity and agglomeration factor.

X-ray diffraction analysis was carried out on a Philips diffractometer equipped with a PW-1720 X-ray source (CuK_α) and a PM-8203 recorder. Silver, palladium and their alloys are known to give fcc crystals. Through Vegard's law, the composition of an Ag/Pd alloy can be deduced from the position of the diffraction peaks.

Two electron microscopes were used: a scanning electron microscope (SEM) JEOL JSM 840 and a transmission electron microscope (TEM) JEOL 2000 EX both equipped with an X-ray microanalysis spectrometer TRACOR Northern® series 2 (lithium-doped silicium diode) providing 149 eV resolution. The minimum analysed surface was 1 μm × 1 μm for the SEM and 15 nm × 15 nm for the TEM. X-ray photoelectron spectrometry (XPS) was carried out on a Leybold-Heraeus spectrometer, and secondary ion mass spectrometry (SIMS) on an IMS 3f CAMECA apparatus, the incident beam being made of Cs^+ ions accelerated by 10 kV.

For XPS and SIMS measurements, the samples were prepared as follows: a small quantity of powder was gently pressed (30 bar) on a tin disc so that the grains were inserted into the tin matrix without being significantly distorted. Thus, in the first layer, the

---

*Also: Laboratoire de Métallurgie Physique, CNRS URA 1107, Bt 413, Université Paris-Sud, 91405 Orsay Cedex, France.

0022–2461 © *1995 Chapman & Hall*

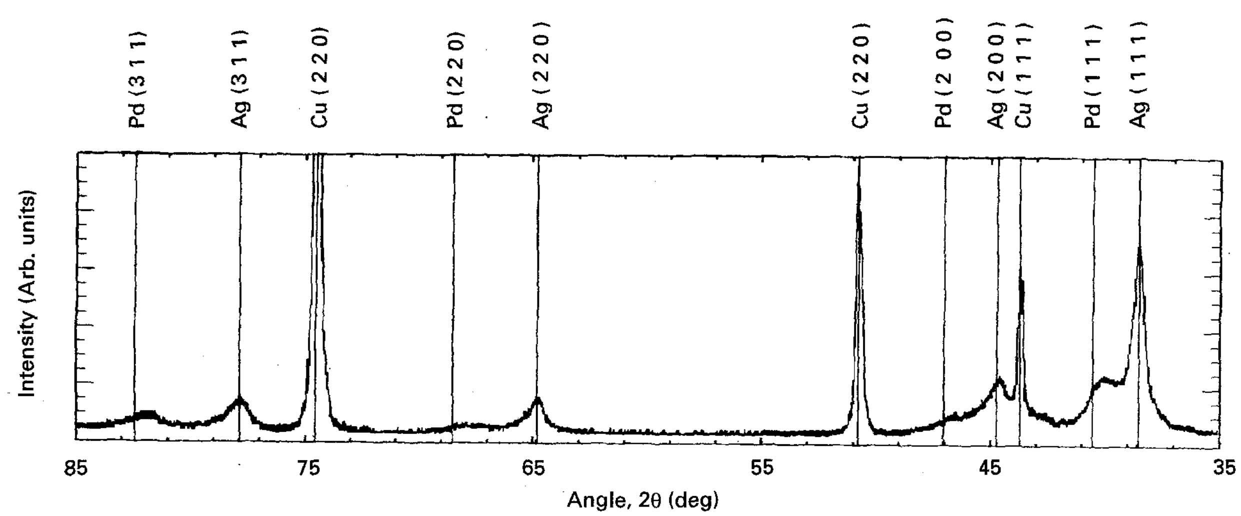

Figure 1 X-ray diffractogram of a 70%/30% Ag/Pd powder: the indexed lines locate the known positions for the pure metals, including copper used as internal calibration.

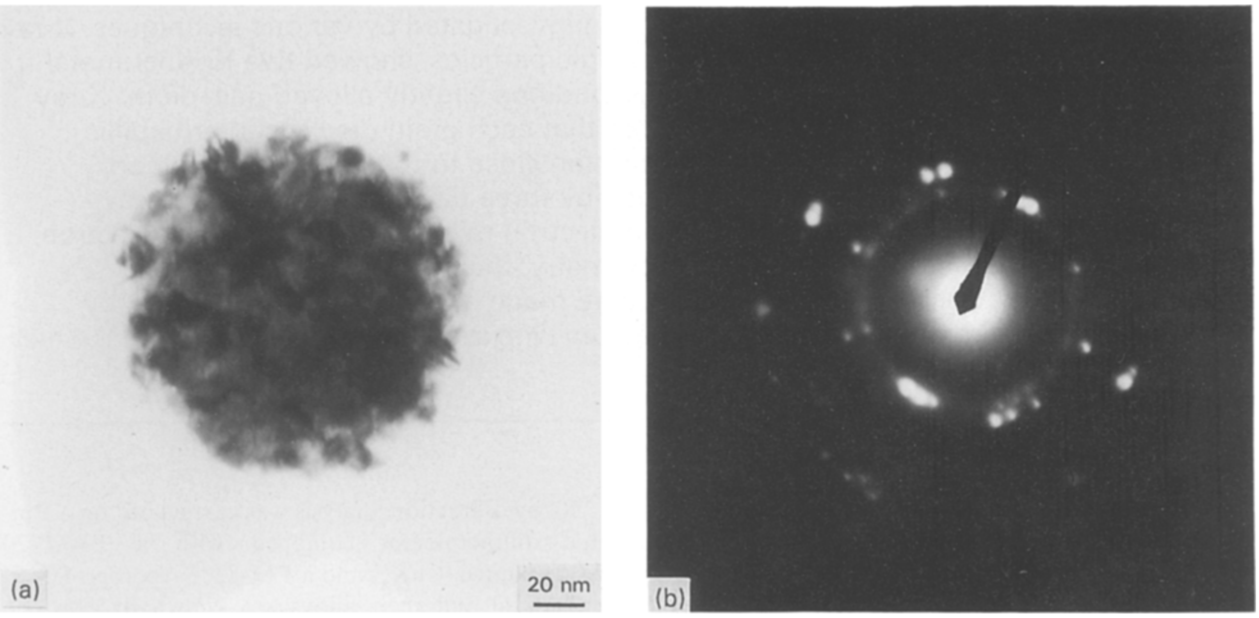

Figure 2 (a) Micrograph and (b) electron diffraction pattern obtained by TEM on an Ag/Pd single particle.

spherical particles are tangential to the external plane (see Fig. 7 below).

3. Results

3.1. Bimetallic character of the powder particles

3.1.1. X-ray diffraction on powders or single particles

Ten powders, prepared with two Ag/Pd ratios and slightly different processing parameters, were studied by X-ray diffraction, all leading to similar results. An example is shown in Fig. 1 for a 70%/30% powder. In addition to copper peaks used for internal calibration purposes, two series of peaks can be easily distinguished: one is constituted of well-defined narrow peaks whose positions coincide with those expected for pure silver; the other is made up of less-intense broader peaks close to those of pure palladium. Therefore, the powder clearly appears to contain two distinct phases: only a weak alloying is observed for the palladium phase.

At this point of the study, two models can be retained: either a mixture of monophase particles, silver grains and palladium grains, each one being pure or almost pure metal; or a powder of bimetallic particles with internal segregation into two distinct phases. Diffraction on a single particle, which has been achieved under TEM, also gives the two series of peaks (Fig. 2) as described above, thus indicating that the first model must be rejected.

3.1.2. X-ray microanalysis under SEM

From the silver and palladium characteristic emission peaks, the relative proportions of the elements can be deduced. Single particles, as well as clusters of several particles, have been analysed: an example is given in Fig. 3. In spite of the proximity of the L_α rays of silver and palladium, the presence of palladium is quite

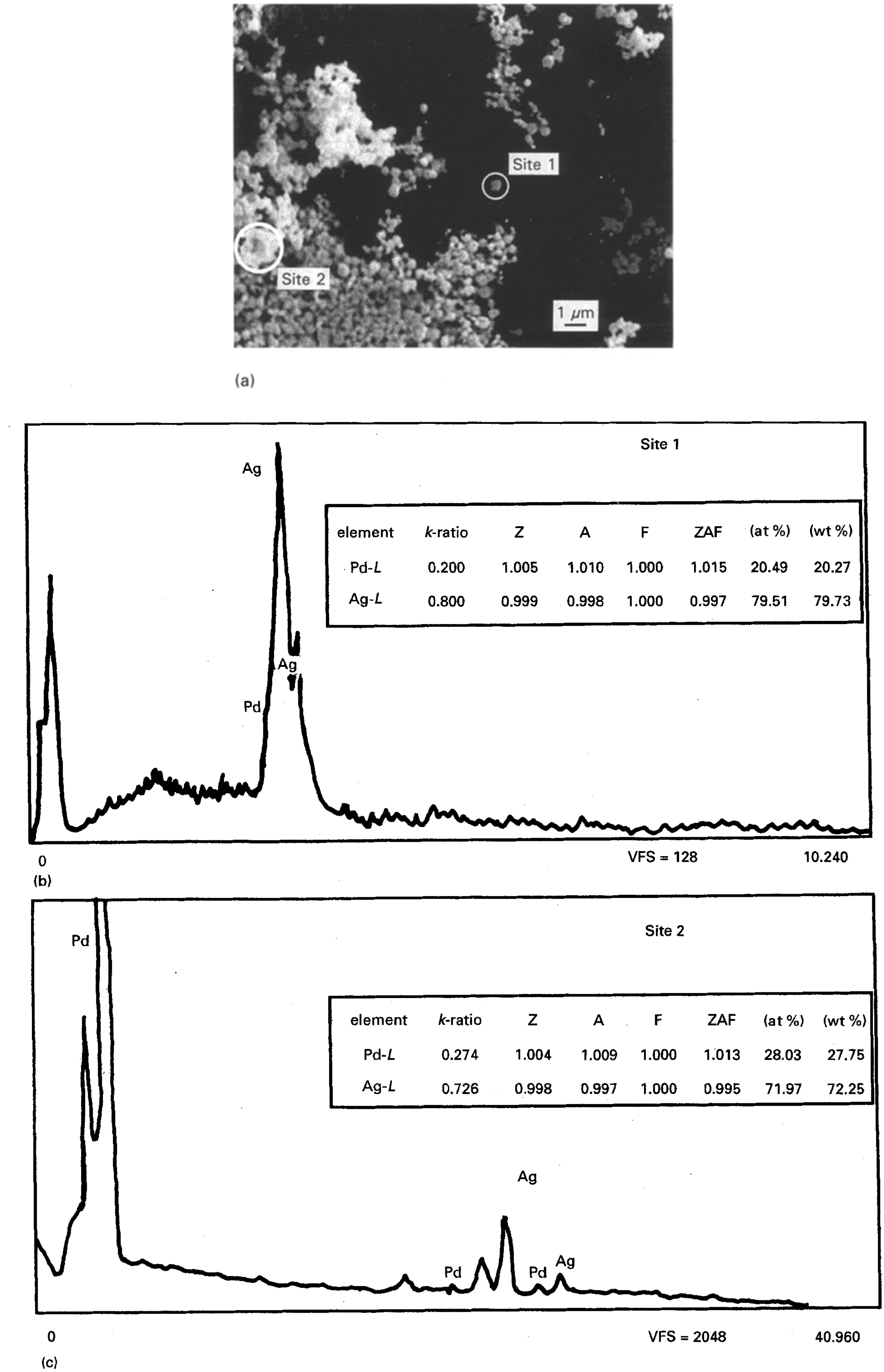

Site 1

element	*k*-ratio	Z	A	F	ZAF	(at %)	(wt %)
Pd-*L*	0.200	1.005	1.010	1.000	1.015	20.49	20.27
Ag-*L*	0.800	0.999	0.998	1.000	0.997	79.51	79.73

Site 2

element	*k*-ratio	Z	A	F	ZAF	(at %)	(wt %)
Pd-*L*	0.274	1.004	1.009	1.000	1.013	28.03	27.75
Ag-*L*	0.726	0.998	0.997	1.000	0.995	71.97	72.25

Figure 3 (a) Micrograph and (b) X-ray microanalysis obtained by SEM on a 75%/25% Ag/Pd powder (15 kV; 40°). Site 1, single particle; Site 2, clustered particle.

certain: in the K_α region, the rays are well energy-separated so that the K_α ray of palladium is clearly observed. The analysis gives about the same proportion for clusters as for single particles within the experimental error: 72%–80% Ag and 28%–20% Pd; this result is close to the mean powder composition (75%/25% in this case). Therefore, these measurements confirm the bimetallic character of each powder particle.

3.2. Space arrangement of silver and palladium metals in the particles

At this step of the study, each particle appeared to be made of two phases, but the techniques used so far did not provide access to the spatial arrangement of silver and palladium inside a particle: in particular, it was not possible to conclude whether the particle included only two domains resulting from a two-step growth, or many more domains possibly resulting from the coalescence of smaller-sized particles. More sophisticated techniques can shed some light on this, as given below.

3.2.1. X-ray microanalysis under TEM

The size of the probe used under the TEM (15 nm × 15 nm), which is noticeably less than the particle size ($\phi \approx 300$ nm), allows a space-resolved analysis on a single particle. Such an analysis has been carried out on 20 different particles. The probe was moved along the diameter of the particle as shown in Fig. 4(a). The palladium percentage (in weight) was measured as a function of the probe position: in every case, the palladium content was found to decrease when moving from the edge to the central region then to increase from the centre to the other edge. Why the palladium content found at any point was relatively high ($\geqslant 40\%$), higher than the mean content, can be explained in two ways: first, the incident electron beam must always cross the surface layer which is palladium rich; second, the spectrometer is adapted to thin planar samples so that, in spite of corrections for absorption and secondary emission, the surface layer is always overestimated.

3.2.2. X-ray photoelectron spectrometry

The XPS technique allows quantitative surface analysis of the elements through the number of electrons extracted from 3*d* levels of both silver and palladium atoms. A progressive abrasion of the surface layer is carried out with an Ar^+ ion beam (0.5 nm min^{-1}) so that the depth–composition profile can be determined. The results are shown in Fig. 5. Silver and palladium signals are both observed at any time with relative intensities changing with depth. These changes are shown in Fig. 6, resulting in a plateau value after 200 min or 100 nm. The initial surface layer appears to be very palladium-rich (Pd/Ag = 89%/11% after correction for the respective cross-sections 9.54 and 10.68). After 10 nm, a progressive enrichment in silver is observed up to the particle core (mean particle diameter 300 nm), thus confirming the model of a silver core surrounded by a palladium-rich alloyed layer ca. 10–15 nm thick. At higher depth (100–200 nm, i.e. 200–400 min), the ratio Ag/Pd is found to be 72%/28%, close to the mean one (75%/25%): at such a depth, the analysed layer is randomized due to the size distribution of the powder particles (Fig. 7).

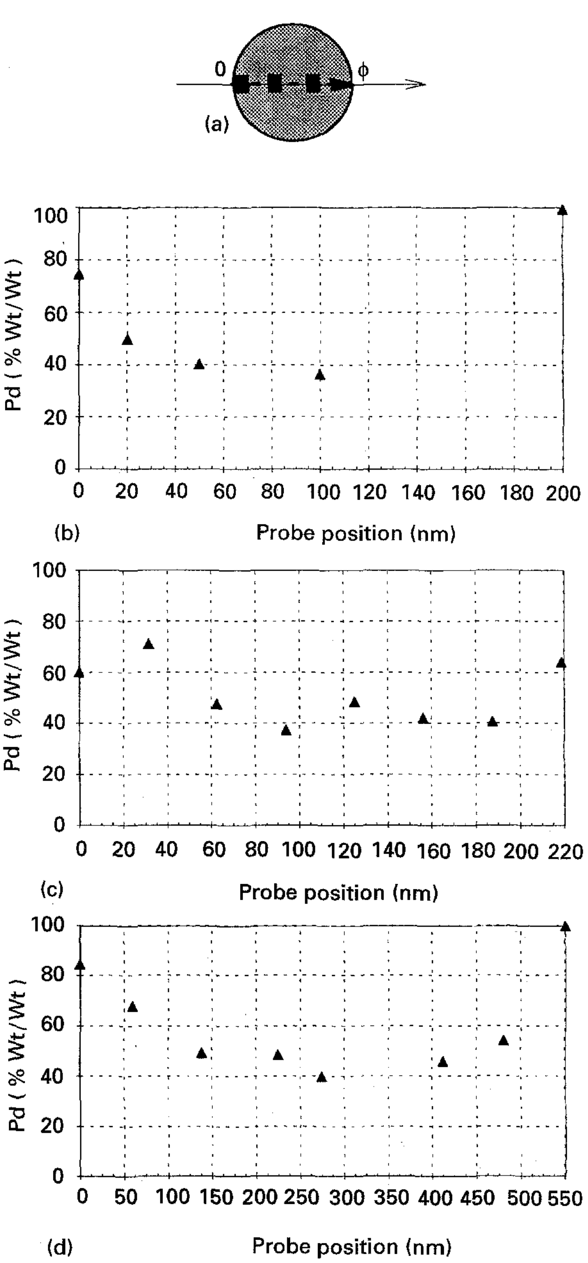

Figure 4 Composition changes along the diameter in single grains of a 75/25 Ag/Pd powder. The probe position is set as shown in (a). (b) $\phi = 200$ nm, (c) $\phi = 220$ nm, (d) $\phi = 550$ nm.

More detailed information can be deduced from the peak positions: both silver and palladium peaks are shifted to higher energies with increasing depth, with a more marked effect for silver. After 150 nm abrasion, which is the mean position of the centres of the first particle layer, the Ag $3d_{5/2}$ peak is exactly at the energy of pure silver which is very well known, because it is commonly used for calibration: the silver shift is a chemical shift assigned to the progressive change from a surface alloy (with a low silver content) to a pure silver core. The shift of the palladium peak,

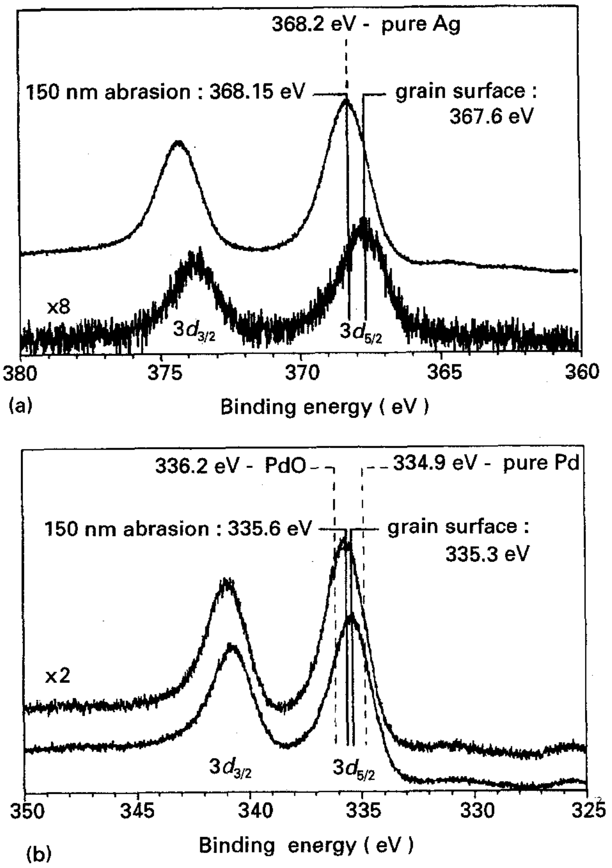

Figure 5 XPS peaks ($3d_{3/2}$ and $3d_{5/2}$) for (a) silver and (b) palladium at the beginning of the run and after 150 nm abrasion. For calibration, the positions of Ag ($3d_{5/2}$) and Pd ($3d_{5/2}$) for pure metals and PdO are marked by dashed lines.

hardly significant, might correspond to a palladium gradient with increasing values for positions close to the particle surface. PdO is not observed because the corresponding shift would be on the opposite side. (However, some oxygen has been detected without any possible quantitative estimation.)

3.2.3. Secondary ion mass spectrometry

The incident Cs^+ beam continuously hits the sample surface: CsM^+ ions (where M is a metal atom taken out from the surface) are formed and then mass analysed. The beam progressively erodes the sample, making it possible to realize depth–profile analysis. Owing to the close atomic weights of silver and palladium, the absolute identification of the peaks is achieved by comparing their intensities with the natural relative abundances of silver and palladium isotopes. A weak signal is obtained for $PdHCs^+$ which can be quantitatively neglected.

Fig. 8 shows the intensities measured for some significant masses, versus the erosion time. The 238 and 243 masses correspond to palladium isotopes ^{105}Pd and ^{110}Pd; the peaks at 240 and 242 are assigned to ^{107}Ag and ^{109}Ag. The measured intensities do not allow quantitative measurements, because the cross-sections are unknown for this material. Only the changes with time (or depth) are significant: the erosion rate (20 nm min^{-1}) is deduced from the hole depth at the end of the experiment, as measured by a profilemeter (inset Fig. 8). The results show that: (i) the surface is richer in palladium than the core, and (ii) some silver is present from the beginning, i.e. at the particle surface, thus confirming the core/rind model. After 20 nm erosion, no oscillations are found as would be expected if the particles were rigoroulsy monodisperse: almost constant signals then correspond to the mean composition of the actual spheres (Fig. 7). From the known value Ag/Pd = 75%/25% of this mean composition, the approximate ratio 12%/

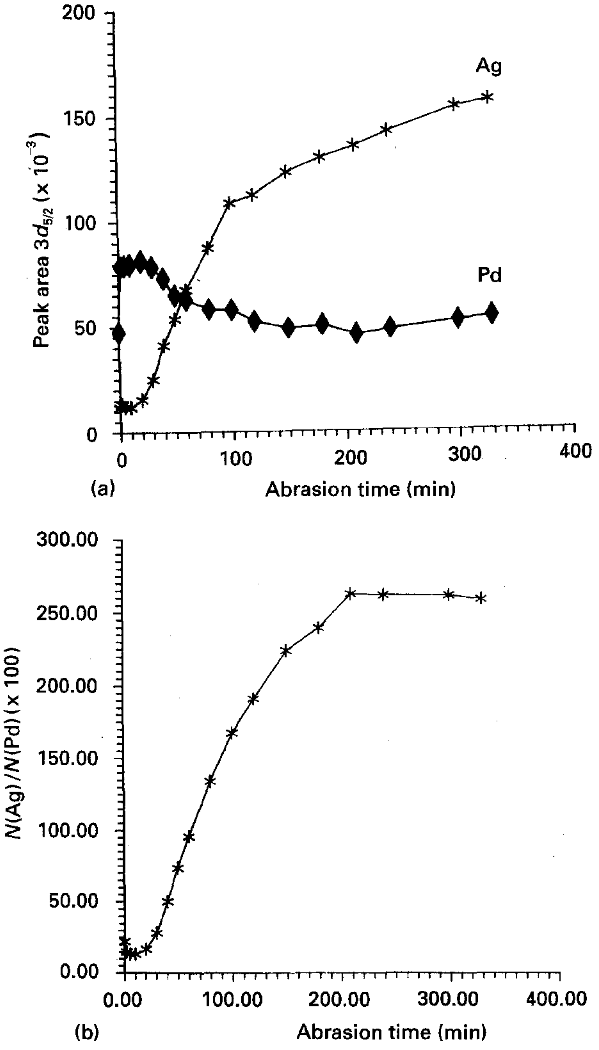

Figure 6 Changes in the Ag/Pd ratio with the abrasion time (argon abrasion rate 0.5 nm min^{-1}): (a) peak area for each metal, (b) relative abundancy corrected for cross-sections (Powder CP543).

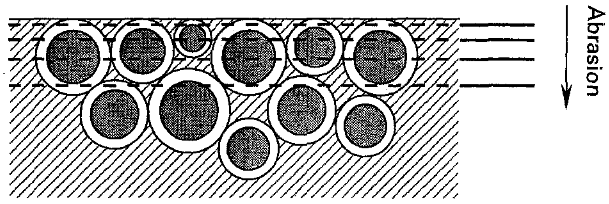

Figure 7 Scheme showing the arrangement of the powder grains in a sample pressed into a tin pellet. In the first layer, the grains are tangential to the sample surface so that the XPS and SIMS analysis first concern the grain rind; then, as abrasion continues, the probe position is more and more randomized.

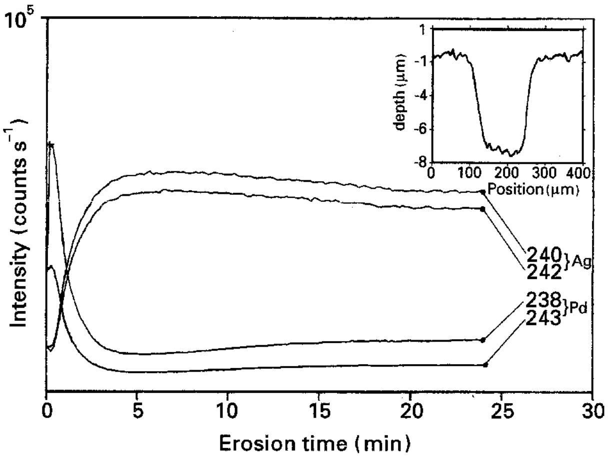

Figure 8 Changes in the ion-beam intensity measured by SIMS for a few relevant masses with erosion time. Insert: crater profile measured with a profilometer.

88% is derived for the surface layer, in agreement with above results.

4. Conclusion

All of the techniques used in this work provide converging information about the structure of the powder particles. Each grain, which is spherical in shape, is shown to be made of a pure silver core surrounded by a 10–15 nm thick alloyed layer with a high palladium content (≈ 89%), possibly higher when closer to the surface. It should be noted that in spite of its biphasic structure, this powder leads to conducting layers with excellent performances (≈ 16 µΩ cm for 2 µm thickness [9]) due to the presence of both metals inside each submicronic grain, so that interdiffusion occurs rapidly when heated.

Acknowledgements

The authors thank J. Philibert and D. Aucouturier for helpful discussions and for providing access to the TEM, XPS and SIMS techniques available in the Laboratoire de Métallurgie Physique, Orsay. They also thank R. Laval, CEETAM, Orsay, for microanalysis measurements in the SEM. This work was financially supported by CLAL and by ADEME (Agence De l'Environnement et la Maîtrise de l'Energie).

References

1. G. G. FERRIER, A. R. BERZINS and N. M. DAVEY, *Platinum Metals Rev.* **29** (1985) 175.
2. L. C. HOFFMANN, *Adv. Ceram.* **19** (1986) 71.
3. K. NAGASHIMA, T. HIMEDA and A. KATO, *J. Mater. Sci.* **26** (1991) 2477.
4. M. H. LA BRANCHE, J. G. PEPIN and W. BORLAND, in "Proceedings of the ASM Thick film Conference", Atlanta, GA, June 1988 (ASM Int., Metals Park, OH).
5. J. G. PEPIN, *J. Mater. Sci. Mater. Electron.* **2** (1991) 34.
6. S. F. WANG and W. HUEBNER, *J. Am. Ceram. Soc.* **74** (1991) 1349.
7. S. F. WANG, W. HUEBNER and C. Y. HUANG, *ibid.* **75** (1992) 2232.
8. D. L. THIEBAULT, in "Precious Metals", edited by A. K. Mehta and R. M. Nadkarni (International Metal Precious Institute; Nielson, Austen, TX, 1992) p. 257.
9. E. DELARUE, M. MOSTAFAVI, M. O. DELCOURT and D. REGNAULT, *J. Mater. Sci.* **30** (1995) p. 628.

Received 23 February
and accepted 27 July 1994